PERGAMON

Journal of Atmospheric and Solar-Terrestrial Physics 64 (2002) 633–638

Journal of ATMOSPHERIC AND SOLAR-TERRESTRIAL PHYSICS

www.elsevier.com/locate/jastp

Using particle simulations for parameter tuning of dynamical models of the magnetotail

I. Doxas[a,*], W. Horton[b], R. Weigel[b]

[a] *Department of Physics, University of Colorado, Boulder, CO 80309-0391, USA*
[b] *Institute for Fusion Studies, The University of Texas at Austin, Austin, TX 78712, USA*

Abstract

WINDMI is a family of dynamical models of the magnetotail that use different closure schemes to derive truncated descriptions of the collisionless microscopic energy transfer processes occurring in the quasineutral layer. The six-dimensional systems are both Kirchhoffian and Hamiltonian in structure, ensuring that the power input from the solar wind is divided into physically realizable energy sub-components. Model parameters are defined analytically as volume integrals of physically identifiable quantities. Particle simulations are used to calculate the parameters for the various models, giving a direct comparison of the relative advantages of different closure schemes. A collisionless kinetic closure scheme that includes the heat flux gives better agreement with observations by allowing for a rapid non-adiabatic cooling of the central plasma sheet (CPS).

Keywords: Magnetotail; Modelling; Simulations; Dynamical systems

1. Introduction

During the past decade of magnetospheric research a clearer understanding has emerged of the collisionless kinetic transport mechanisms for the passage of energy and momentum through the nightside magnetotail to the ionosphere. The improved understanding of the energy-momentum transport has resulted from the combined use of nonlinear dynamics theory coupled with large-scale computer simulations for ensembles of plasma particles. Both test particle (e.g. Ashour-Abdalla et al., 1994; Chen, 1992; Speiser and Martin, 1992; Doxas et al., 1990, 1994) and self-consistent simulations (e.g. Winske, 1981; Winglee and Steinolfson, 1993; Pritchett, 1994), when interpreted with nonlinear theory, provide the tools for formulating transport formulas for the critical zones such as the quasineutral plasma sheet in the geomagnetic tail. In the central plasma sheet (CPS) the ion orbits are complex and chaotic as measured by the local exponential divergence of neighboring orbits (e.g. Chen and Palmadesso, 1986; Büchner and Zelenyĭ, 1986, 1987; Chen, 1992). In this boundary layer there is strong energization of the ions while the electrons remain magnetized (Lyons and Speiser, 1982; Horton and Tajima, 1990, 1991a; Baek et al., 1995; Usadi et al., 1986). On the scale of the collisionless skin depth (< 100 km) the electrons also become detached from the magnetic field and are energized (Pritchett and Coroniti, 1995).

In addition to the new understanding of the basic physics of the energization processes in the CPS, there have been important advances made in methods for analyzing the correlated structures in input–output time series for the underlying dynamics (cf. Klimas et al., 1996 and references therein). Thus, a powerful alternative to the classical electromagnetic modeling is the development of physics-based dynamical models and linear and nonlinear prediction filters, which have been demonstrated to have high predictive capacity for a wide range of magnetospheric parameters (e.g. Horton and Doxas, 1996, 1998; Bargatze et al., 1985; Sharma et al., 1993; Hernández et al., 1993; Vassiliadis et al., 1995; Klimas et al., 1992, 1994, 1996, 1997).

* Corresponding author.
E-mail address: doxas@colorado.edu (I. Doxas).

1364-6826/02/$ - see front matter © 2002 Published by Elsevier Science Ltd.
PII: S1364-6826(02)00022-6

2. A physics based dynamical model

WINDMI is a physics based model for the coupled solar wind–Magnetosphere–Ionosphere system (Horton and Doxas, 1996, 1998). It couples the four basic energy components of the nightside magnetosphere:

1. Magnetic field energy:

$$W_{\mathrm{B}} = \int \frac{B^2}{2\mu_0}\,\mathrm{d}^3x = \frac{1}{2}\,\mathscr{L}I^2 + \frac{1}{2}\,\mathscr{L}_{\mathrm{I}}I_{\mathrm{I}}^2 - MII_1. \tag{1}$$

2. $\mathbf{E}\times\mathbf{B}$ kinetic energy:

$$K_{\perp} = \int \frac{1}{2}\,\rho_{\mathrm{m}}u_{\mathrm{E}}^2\,\mathrm{d}^3x = \frac{1}{2}\,CV^2 + \frac{1}{2}\,C_{\mathrm{I}}V_{\mathrm{I}}^2. \tag{2}$$

3. Parallel kinetic energy:

$$K_{\parallel} = \int_{\mathrm{CPS+PSBL}} \frac{1}{2}\,\rho_{\mathrm{m}}u_{\parallel}^2\,\mathrm{d}^3x. \tag{3}$$

4. Thermal energy:

$$U = \int_{\mathrm{CPS}} \left(P_{\perp} + \frac{1}{2}\,P_{\parallel}\right)\mathrm{d}^3x \cong \frac{3}{2}\,P_0\Omega \tag{4}$$

to the ionosphere via the nightside region 1 currents. Eqs. (1) and (2) serve as the definitions of the inductances and capacitances associated with current loops and electric potentials (e.g. Horton et al., 1998; Doxas et al., 1999). The thermal energy, U, is replaced by the mean pressure, $P_0(t)$, within a fixed volume $\Omega_{\mathrm{CPS}} = L_xL_yL_z$ of the CPS. The model is a six-dimensional 13-parameter system, given by

$$\mathscr{L}\frac{\mathrm{d}I}{\mathrm{d}t} = V_{\mathrm{sw}}(t) - V + M\frac{\mathrm{d}I_1}{\mathrm{d}t}, \tag{5}$$

$$C\frac{\mathrm{d}V}{\mathrm{d}t} = I - I_1 - I_{\mathrm{ps}} - \Sigma V, \tag{6}$$

$$\frac{3}{2}\frac{\mathrm{d}P}{\mathrm{d}t} = \Sigma\frac{V^2}{\Omega} - u_0K_{\parallel}^{1/2}\Theta(I - I_{\mathrm{c}})P, \tag{7}$$

$$\frac{\mathrm{d}K_{\parallel}}{\mathrm{d}t} = I_{\mathrm{ps}}V - \frac{K_{\parallel}}{\tau_{\parallel}}, \tag{8}$$

$$\mathscr{L}_{\mathrm{I}}\frac{\mathrm{d}I_1}{\mathrm{d}t} = V - V_{\mathrm{I}} + M\frac{\mathrm{d}I}{\mathrm{d}t}, \tag{9}$$

$$C_{\mathrm{I}}\frac{\mathrm{d}V_{\mathrm{I}}}{\mathrm{d}t} = I_1 - \Sigma_{\mathrm{I}}V_{\mathrm{I}}. \tag{10}$$

The quantities $\mathscr{L}$, C, Σ, $\mathscr{L}_{\mathrm{I}}$, C_{I}, and Σ_{I} are the magnetospheric and ionospheric inductance, capacitance, and conductance, respectively. M is the mutual inductance between the lobe current, I, and the region 1 current, I_1 (cf. Horton and Doxas, 1998). The pressure gradient driven current is given by $I_{\mathrm{ps}}(t) = \alpha P^{1/2}(t)$ as derived from $\mathbf{j}\times\mathbf{B} = \nabla P$ force balance and Ampére's law. The parameter α is an average over the pressure profile in the current sheet. The solar wind driving voltage in Eq. (5) is given $V_{\mathrm{sw}} = \beta_{\mathrm{sw}}V_x^{\mathrm{sw}}B_s^{\mathrm{IMF}}L_y$, where β_{sw} reflects the efficiency with which the solar wind electromotive force is translated into a cross-tail potential drop (cf. Goertz et al., 1993). The solar wind voltage $V_{\mathrm{sw}}(t)$ is the input time series for this nonlinear driven-dissipative system. The term $u_0K_{\parallel}^{1/2}\Theta(I - I_{\mathrm{c}})P$ represents the rapid unloading of the stored energy when the current exceeds a critical value, I_{c}, and comes from the heat flux limit that is neglected in the MHD closure (Horton and Doxas, 1996). The system is kirchhoffian, ensuring that charge and energy are conserved. The non-dissipative components of the six coupling terms are hamiltonian, ensuring that the solar wind input is subdivided into physically realizable subcomponents. In the absence of driving and in the dissipationless limit the total energy is conserved $(\mathrm{d}/\mathrm{d}t[K_{\perp} + K_{\parallel} + W_{\mathrm{B}} + U] = 0)$. Most parameters of the model can be calculated from their integral definitions (see Horton and Doxas, 1996, 1998; Horton et al., 1998; Doxas et al., 1999) providing a consistent mathematical formalism into which different models of critical subsystems can be inserted and evaluated.

The dynamical system described by Eqs. (5)–(10) is derived from the Vlasov equation with a heat-flux limit closure scheme (Horton and Doxas, 1996). The moments of the Vlasov equation for species of index a give:

$$\frac{\partial n_a}{\partial t} + \nabla\cdot(n_a\mathbf{u}_a) = 0, \tag{11}$$

$$m_an_a\left(\frac{\partial}{\partial t} + \mathbf{u}_a\cdot\nabla\right)\mathbf{u}_a = n_ae_a(\mathbf{E} + \mathbf{u}_a\times\mathbf{B}) - \nabla P_a - \nabla\cdot\boldsymbol{\pi}_a, \tag{12}$$

$$\frac{3}{2}\frac{\partial P_a}{\partial t} + \nabla\cdot(\mathbf{q}_a + \tfrac{5}{2}P_a\mathbf{u}_a + \mathbf{u}_a\cdot\boldsymbol{\pi}_a) - \mathbf{u}_a\cdot\nabla P_a = \mathbf{u}_a\cdot\nabla\cdot\boldsymbol{\pi}_a, \tag{13}$$

where closure requires a specification of the thermal flux $\mathbf{q}_a$ in terms of $n_a, \mathbf{u}_a, P_a$. In the MHD closure, the simplifications are (i) neglect the divergence of the heat flux $\nabla\cdot\mathbf{q} = 0$ (ii) drop the off-diagonal momentum flux $\boldsymbol{\pi}_a = 0$, (iii) neglect the diamagnetic flow velocities $v_{\mathrm{di}} = (\rho_{\mathrm{i}}/L)v_{\mathrm{i}}$ compared to the MHD velocity $E_{\perp}/B$, and (iv) neglect the electron inertia $m_{\mathrm{e}}/m_{\mathrm{i}} \to 0$. In the central plasma sheet the local ion gyroradius parameter $\varepsilon = \rho_{\mathrm{i}}\max(\partial B/B\partial x) \sim \rho_{\mathrm{i}}/R_{\mathrm{c}}$ becomes large and assumptions (i) through (iii) fail. The essential non-MHD physics included in the model is given by

(a) The collisionless transport for the geomagnetic tail, which appears in the finite value of $\mathbf{u}_{\mathrm{i}}\cdot\nabla\cdot\boldsymbol{\pi}_{\mathrm{i}}$ that transfers energy between Eqs. (12) and (13) and provides an irreversible energization of the ions. The large ion gyroradius conductivity gives a finite conductance Σ and non-adiabatic ion thermalization in the quasineutral sheet $\Delta Z = (\rho_{\mathrm{i}}L)^{1/2}$ which vanishes in the MHD limit. The conductivity

was derived from theory and test particle simulations (Horton and Tajima, 1991a,b) and contains the Lyons and Speiser (1982) energization mechanism for the transient ions as part of the ensemble average over the modified Harris sheet equilibrium.

(b) The kinetic loss rate of thermal energy. We model the outflow terms by

$$q_n \simeq Pu_n = Pu_{\|} \simeq P(2K_{\|}/m_i)^{1/2} \equiv u_0 P K_{\|}^{1/2} \tag{14}$$

(Horton and Doxas, 1996) so the thermal energy loss rate is described by the parallel heat flux, represented by the heat flux limit parameter u_0, and the mean parallel flow velocity associated with the MHD parallel flow kinetic energy, $K_{\|}(t)$. The Geotail particle data, currently being analyzed with respect to the parallel thermal flux by Hoshino et al. (1998), show that the minimum ratio of the thermal plasma energy density P to the kinetic energy density $(1/2)\rho v^2$ found in the central plasma sheet is consistent with a parallel heat flux taken as a fraction of $Pv_{\|}$.

WINDMI can be used as a nonlinear prediction filter, with parameter values determined by a global minimization procedure over a predetermined set of "training" data. An example of this is given in Horton and Doxas (1998), where the average relative variance (ARV) of the WINDMI output was minimized over the Bargatze et al. (1985) dataset using one-dimensional sweeps in four of the parameters, L, Σ, C, and β_{sw}. However, although informative, use of WINDMI as a prediction filter with global coefficients is not very fruitful, since data driven prediction filters have better forecasting capabilities. WINDMI's main advantage is that it can provide insight into the physical processes that determine magnetospheric dynamics. Most of the parameters in WINDMI can be calculated from their integral definitions, the only exceptions being the coupling to the solar wind, and the ionospheric dissipation. These are the model's "boundary conditions", being the energy source and sink respectively; in the absence of driving and in the dissipationless limit WINDMI conserves energy (Horton and Doxas (1996, 1998); the magnetotail conductivity is non-dissipative, see Horton and Tajima (1991a,b)). Detailed examples of how different parameters are calculated are given in Horton et al. (1998) for the inductances (L, L_1, and M), in Horton and Doxas (1998) for the ionospheric conductivity, and in Doxas et al. (1999) for the capacitance. Horton and Tajima (1991a, b) show a detailed calculation of the non-dissipative tail conductivity Σ.

WINDMI therefore presents a consistent mathematical framework in which different models of critical subsystems can be inserted and evaluated. A study of the ionospheric conductivity for instance shows that the Robinson et al. (1987) formula relating ionospheric conductivity to the power dissipated in the ionosphere gives better agreement with observations (Horton and Doxas, 1998). In this paper, we show that the non-MHD closure used in the model gives better agreement with observations by allowing for a fast non-adiabatic cooling of the CPS through the heat flux term which is neglected by the MHD closure. The results are consistent with guiding center theory which requires that plasma parameters vary slowly along the magnetic field for the heat flux to be negligible (e.g. Kulsrud, 1983; Sugama et al., 2001).

3. Using particle simulations to tune model parameters

In comparing the response of the dynamical model to the Blanchard–McPherron dataset of isolated events (Blanchard and McPherron, 1995), we find that we get better agreement with observations if we couple the model to the results of test particle simulations (Doxas et al., 1999). The simulations provide the moments of the distribution function that can be used to calculate the parameters of the model using their integral definitions (Horton and Doxas, 1996). The parameters that can be calculated using a numerically provided distribution function are the capacitance and conductance of the CPS, C and Σ, the unloading parameter, u_0 (which is related to the heat flux through Eq. (14)), and the pressure gradient driven current I_{ps}, which is defined in terms of the average pressure over the CPS ($I_{ps} = \alpha \Omega_{CPS}^{-1} \int_{\Omega_{CPS}} P_i \, d^3x$). Of these, explicit calculations using particle simulations have been made for C and u_0, while all other parameters values are held constant. The conductance and pressure gradient driven current will be investigated using particle simulations in future work.

The simulations use a time-dependent model for the magnetotail fields, consisting of a tearing mode superimposed on a two-dimensional Harris sheet:

$$B_x = B_0 \tanh\left(\frac{z}{L_z}\right), \quad B_z = B_0 b_0 + B_0 \psi_0 k \sin(kx) e^{\gamma t}. \tag{15}$$

Fig. 1a shows the model fields and a sample 1000 particles superimposed. The number of particles in the simulations varies from 2×10^5 to 2×10^6, the lobe field is $B_0 = 20$ nT, the ratio of northward to horizontal field, b_0 varies from 10 to 40, the wavelength of the perturbation varies from 10 to 50 R_E, and the tearing mode growth rate varies from 0.03/s to 0.001/s. Although obtaining higher order moments like the heat flux requires a larger number of particles, lower order moments obtained with these simulations (density, velocity, and temperature) have been extensively studied and are in good agreement with observations (Doxas et al., 1990, 1993, 1994).

The particles are advance in the fields (15) until the current sheet attains its minimum thickness, the heat flux is calculated using the numerical particle distribution function, and the result is used to calculate the flux limit parameter u_0 (Eq. (14)). Fig. 1a clearly shows that the particle density at least is not a slowly varying quantity, violating the strict condition for neglecting the heat flux (e.g. Kulsrud, 1983). Most plasma parameters also have steep changes around the

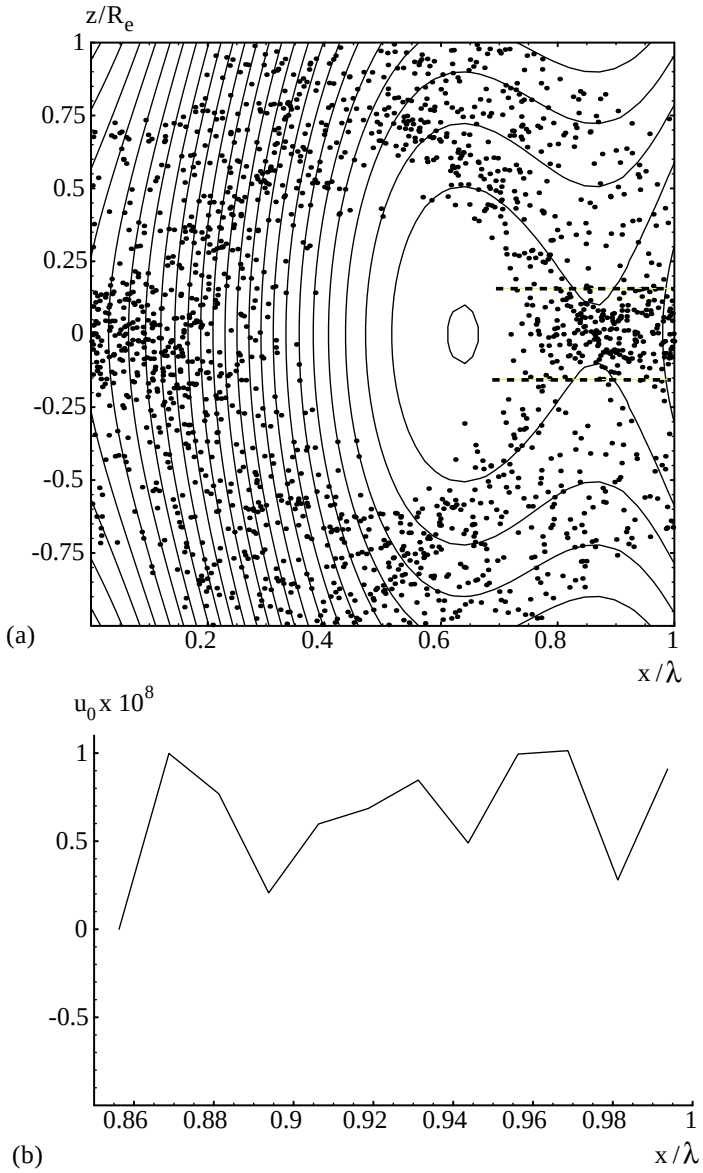

Fig. 1. (a) The model fields, Eq. (15), for the particle simulations with a sample 1000 particles superimposed. The dashed lines show the location where u_0 is calculated. (b) The unloading factor, u_0 (Eq. (19)), calculated at the upper dashed line shown in (a) and averaged over six cell transit times.

reconnection region (e.g. Doxas et al., 1994) violating the condition of slow variation along the field.

The moments and fluxes at a cell (m,n) are given by

$$\mathbf{u}_{m,n} = \frac{1}{N_{m,n}} \sum_{i=1}^{N_{m,n}} \mathbf{v}_i, \tag{16}$$

$$P_{m,n} = \frac{m_i}{3} \left[\frac{1}{N_{m,n}} \sum_{i=1}^{N_{m,n}} (\mathbf{v}_i - \mathbf{u}_{m,n})^2 \right], \tag{17}$$

$$\mathbf{q}_{m,n} = \frac{m_i}{2} \left[\frac{1}{N_{m,n}} \sum_{i=1}^{N_{m,n}} (\mathbf{v}_i - \mathbf{u}_{m,n})^2 (\mathbf{v}_i - \mathbf{u}_{m,n}) \right], \tag{18}$$

where $N_{m,n}$ is the number of particles in the cell (m,n). The unloading parameter, u_0, is then calculated via Eq. (14) using the numerically obtained values of $\mathbf{q}$, P, and $\mathbf{v}_{\|} \sim \sqrt{K_{\|}}$ by averaging over all the cells at the boundary of the CPS (dashed lines in Fig. 1a) and over a number of timesteps, typically of the order of ten. The time averaging is performed in order to increase the number of particles in the calculation,

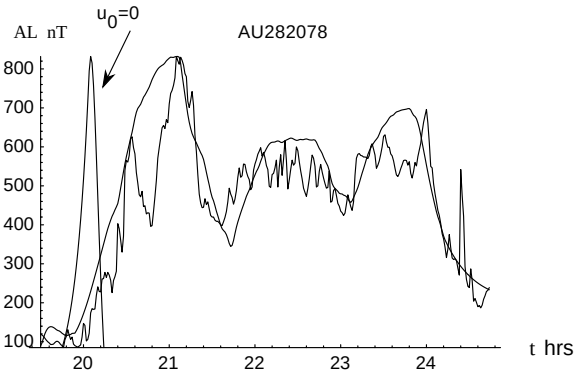

Fig. 2. The results of the dynamical model compared to the AL index for one of the isolated events in the Blanchard–McPherron database. The flux limit term u_0 in Eq. (7) was calculated using particle simulations. When the thermal flux term is neglected ($q = 0 \Rightarrow u_0 = 0$) the model gives an unphysical short spike followed by large amplitude ringing (the negative values of the ringing are suppressed to increase the clarity of the figure). The unphysical response is due to the inability of the central plasma sheet to cool non-adiabatically in the absence of a heat flux term.

and the values that are used are separated by at least two transit times (the time it takes a particle to cross a cell) to insure that the measurements include independent values.

From the above equations, we see that the kinetic closure consists of expressing the third-order moment **q** in terms of the lower order moments P and **v**. This closure scheme is supported by Geotail particle data, currently being analyzed with respect to the parallel thermal flux (Hoshino et al., 1998). The unloading parameter, u_0, is therefore given by

$$u_0 = \sqrt{K_r}\,\frac{\langle (v - \langle v\rangle)^2 (v_\parallel - \langle v_\parallel\rangle)\rangle}{\langle (v - \langle v\rangle)^2\rangle \langle v_\parallel\rangle}, \tag{19}$$

where the averaging is performed over the particles in the simulation (Eqs. (16)–(18)), and K_r is the ratio of total parallel kinetic energy in the tail (Eq. (3)) to that in the simulation, $(1/2)m\Sigma v_i^2$ (typically $K_r \sim 10^{20}$). Fig. 1b shows u_0 as a function of x for a typical simulation.

Fig. 2 shows the results for one of the events in the Blanchard and McPherron (1995) database of isolated events. We see that including the heat flux term gives good agreement with the measured AL index, while the predictions of the model without the heat flux limit give an unphysical large short spike. This is due to the fact that without a heat loss term the system (5)–(10) has no mechanism for cooling the CPS plasma non-adiabatically, resulting in an unphysical built-up of energy. We therefore see that by including the heat flux term, the model allows for the rapid unloading of plasma sheet thermal energy, an effect not allowed by the MHD closure scheme.

4. Conclusions

A physics based model of the coupled magnetotail-ionosphere (Horton and Doxas, 1998) is used as an input–output filter, and its performance is compared to the Blanchard–McPherron database of isolated events. Most model parameters can be calculated analytically for different substorm scenarios and closure schemes. The fact that the performance of the model improves significantly when a closure scheme that includes the heat flux is used, demonstrates how the dynamical model can provide us with insight into the physics of the magnetosphere. Although considerable work still remains to be done, it is clear that the dynamical model provides a method for discriminating between different proposed substorm mechanisms. The model's predictive performance is still inferior to that of data based filters, but the results have a direct physical interpretation for the state of the magnetosphere.

References

Ashour-Abdalla, M., Zelenyĭ, L.M., Peroomian, V., Richard, R.L., 1994. Consequences of magnetotail ion dynamics. Journal of Geophysical Research 99, 14,891.

Baek, S.-C., Choi, D.-J., Horton, W., 1995. Dawn-dusk magnetic field effects on ions accelerated in the current sheet. Journal of Geophysical Research 100, 14,935.

Bargatze, L.F., Baker, D.N., McPherron, R.L., Hones Jr., E.W., 1985. Magnetospheric impulse response for many levels of geomagnetic activity. Journal of Geophysical Research 90, 6387.

Blanchard, G.T., McPherron, R.L., 1995. Analysis of the linear response function relating AL to VBs for individual substorms. Journal of Geophysical Research 100, 19,155.

Büchner, J., Zelenyĭ, L.M., 1986. Deterministic chaos in the dynamics of charged particles near a magnetic field reversal. Physics Letters A 118, 395.

Büchner, J., Zelenyĭ, L.M., 1987. Chaotisation of the electron motion as the cause of an internal magnetotail instability and substorm onset. Journal of Geophysical Research 92, 13,456.

Chen, J., Palmadesso, P., 1986. Chaos and nonlinear dynamics of single-particle orbits in a magnetotail-like magnetic field. Journal of Geophysical Research 91, 1499.

Chen, J., 1992. Nonlinear dynamics of charged particles in the magnetotail. Journal of Geophysical Research 97, 15,011.

Doxas, I., Horton, W., Sandusky, K., Tajima, T., Steinfolson, R., 1990. Numerical study of the current sheet and plasma sheet boundary layer in a magnetotail model. Journal of Geophysical Research 95, 12,033.

Doxas, I., Burkhart, G., Speiser, T.W., Dusenbery, P.B., 1993. Stochastic plasma heating by a neutral line. In: Chen, T., Crew, G.B., Jasperse, J.R. (Eds.), Physics of Space Plasmas, Vol. 247. Scientific Publishers, Inc., Cambridge, MA.

Doxas, I., Speiser, T.W., Dusenbery, P.B., Horton, W., 1994. A proposed neutral line signature. Journal of Geophysical Research 99, 2375.

Doxas, I., Horton, W., Smith, J.P., 1999. A physics based nonlinear dynamical model for the solar wind driven magnetosphere–ionosphere system. Physics and Chemistry of the Earth 94, 67.

Goertz, C.K., Lin-Hua Shan, , Smith, R.A., 1993. Prediction of geomagnetic activity. Journal of Geophysical Research 98, 7673.

Hernández, J., Tajima, T., Horton, W., 1993. Neural net forecasting for geomagnetic activity. Geophysical Research Letters 20, 2707.

Horton, W., Tajima, T., 1990. Decay of correlations and the collisionless conductivity in the geomagnetic tail. Geophysical Research Letters 17, 123.

Horton, W., Tajima, T., 1991a. Collisionless conductivity and stochastic heating of the plasma sheet in the geomagnetic tail. Journal of Geophysical Research 96, 15,811.

Horton, W., Tajima, T., 1991b. Transport from chaotic orbits in the geomagnetic tail. Geophysical Research Letters 18, 1583.

Horton, W., Doxas, I., 1996. A low dimensional energy conserving state space model for substorm dynamics. Journal of Geophysical Research 101, 27,223.

Horton, W., Doxas, I., 1998. A low-dimensional dynamical model for the solar wind driven geotail-ionosphere system. Journal of Geophysical Research 103A, 4561.

Horton, W., Pekker, W., Doxas, I., 1998. Magnetic energy storage and the nightside magnetosphere–ionosphere coupling. Geophysical Research Letters 25, 4083.

Hoshino, M., Mukai, T., Yamamoto, T., 1998. Ion dynamics in magnetic reconnection: Comparison between numerical simulations and Geotail observations. Journal of Geophysical Research 103, 4509.

Klimas, A.J., Baker, D.N., Roberts, D.A., Fairfield, D.H., Büchner, J., 1992. A nonlinear analog model of geomagnetic activity. Journal of Geophysical Research 97, 12,253.

Klimas, A.J., Baker, D.N., Vassiliadis, D., Roberts, D.A., 1994. Substorm recurrence during steady and variable solar wind driving: evidence of a normal mode in the unloading dynamics of the magnetosphere. Journal of Geophysical Research 99, 14,855.

Klimas, A.J., Vassiliadis, D., Baker, D.N., Roberts, D.A., 1996. The organized nonlinear dynamics of the magnetosphere. Journal of Geophysical Research 101, 13,089.

Klimas, A.J., Vassiliadis, D., Baker, D.N., 1997. Data-derived analogues of the magnetospheric dynamics. Journal of Geophysical Research 102, 26,993.

Kulsrud, R.M., 1983. MHD Description of Plasma. In: Rosenbluth, M.N., Sagdeev, R.Z. (Eds.), Handbook of Plasma Physics, Vol. I, North-Holland Publishing Company, New York.

Lyons, L.R., Speiser, T.W., 1982. Evidence for current sheet acceleration in the geomagnetic tail. Journal of Geophysical Research 87, 2276.

Pritchett, P.L., 1994. Effect of electron dynamics on collisionless reconnection in two dimensional magnetotail equilibrium. Journal of Geophysical Research 99, 5935.

Pritchett, P.L., Coroniti, F.V., 1995. The formation of thin current sheets during plasma sheet convection. Journal of Geophysical Research 100, 23,551.

Robinson, R.M., Vondrak, R.R., Miller, K., Dabbs, T., Hardy, D., 1987. On calculating ionospheric conductances from the flux and energy of precipitating electrons. Journal of Geophysical Research 92, 2565.

Sharma, A.S., Vassiliadis, D.V., Papadopoulos, K., 1993. Reconstruction of low-dimensional magnetospheric dynamics by singular spectrum analysis. Geophysical Research Letters 20, 335.

Speiser, T.W., Martin Jr., R.F., 1992. Energetic ions as remote probes of X-type neutral lines in the geomagnetic tail. Journal of Geophysical Research 97, 10,775.

Sugama, H., Watanabe, T.H., Horton, W., 2001. Collisionless kinetic-fluid closure and its application to the ITG driven system, Physics of Plasmas 8, 2617.

Usadi, A., Wolf, R.A., Heinemann, M., Horton, W., 1986. Does Chaos alter the ensemble-averaged drift equations? Journal of Geophysical Research 101, 15,491.

Vassiliadis, D., Klimas, A.J., Baker, D.N., Roberts, D.A., 1995. A description of the solar wind-magnetosphere coupling based on nonlinear filters. Journal of Geophysical Research 100, 3495.

Winglee, R.M., Steinolfson, R.S., 1993. Energy storage and dissipation in the magnetotail during substorms. 1. Particle simulations. Journal of Geophysical Research 98, 7519.

Winske, D., 1981. Current-driven microinstabilities in a neutral sheet. Physics of Fluids 24, 1069.